Molecular Biology of the Cell
Vol. 3, 1141–1154, October 1992

Modulation of the Dynamic Instability of Tubulin Assembly by the Microtubule-Associated Protein Tau

D.N. Drechsel,* A.A. Hyman,† M.H. Cobb,‡ and M.W. Kirschner*

*Department of Biochemistry and Biophysics and †Pharmacology, University of California, San Francisco, California 94143; and ‡Department of Pharmacology, University of Texas Southwestern Medical Center, Dallas, Texas 75235

Submitted June 19, 1992; Accepted August 3, 1992

Microtubule-associated proteins (MAP), such as tau, modulate the extent and rate of microtubule assembly and play an essential role in morphogenetic processes, such as axonal growth. We have examined the mechanism by which tau affects microtubule polymerization by examining the kinetics of microtubule assembly and disassembly through direct observation of microtubules using dark-field microscopy. Tau increases the rate of polymerization, decreases the rate of transit into the shrinking phase (catastrophe), and inhibits the rate of depolymerization. Tau strongly suppresses the catastrophe rate, and its ability to do so is independent of its ability to increase the elongation rate. Thus, tau generates a partially stable but still dynamic state in microtubules. This state is perturbed by phosphorylation by MAP2 kinase, which affects all three activities by lowering the affinity of tau for the microtubule lattice.

INTRODUCTION

During development, neuroblasts mature, become polarized, and extend long axonal processes. This morphogenesis is accompanied by growth and a dynamic reorganization of the cytoskeleton, including the microtubules that increase greatly in mass and rearrange to form tight parallel bundles within the axons. Besides providing stability for neuronal form, these bundles present tracks for vesicular transport to the distant tip of the axon. This rearrangement is thought to drive outgrowth because addition of inhibitors of microtubule assembly to embryonic cells prevents axonal extension and causes retraction of pre-existing neurites (Yamada *et al.*, 1970; Daniels, 1972). The mechanisms that regulate this rearrangement of the microtubule array remain obscure.

Both in vitro and in cells, tubulin exhibits an unusual polymerization property, termed dynamic instability, which supports the rapid and extensive rearrangements in the microtubule array (Mitchison and Kirschner, 1984; Schulze and Kirschner, 1986). Dynamic instability describes behavior where microtubules alternate between prolonged periods of polymerization and depolymerization. After a random period of growth, a microtubule can begin to shrink (termed catastrophe) and a shrinking microtubule can stochastically resume growth (termed rescue). This leads to a rapid exchange between tubulin polymer and monomer pools and quick and extensive turnover of the microtubule array. In fibroblasts, most microtubules turn over in 10 min (Schulze and Kirschner, 1986). The dynamic nature of the microtubule array permits rapid changes in cell shape, for instance, during axonal extension by neurons, but little is known about how the cell controls these dynamics to achieve final function and form.

Microtubule-associated proteins (MAPs)[1] are attractive candidates for regulation of the reorganization of the microtubule array because in neurons their expression coincides with neurite outgrowth (Drubin *et al.*, 1985; Black *et al.*, 1986). Early studies of mammalian brain microtubules identified the MAP, tau, as a prominent and potent promoter of tubulin assembly in vitro (Cleveland *et al.*, 1977a). Tau promoted nucleation and stimulated both the rate and the extent of microtubule polymer assembly. This property suggested that tau may drive the changes in the growth of the axonal microtubule array. Indeed the importance of tau in nerve cell

[1] *Abbreviations used:* CAM, Ca^{2+}/calmodulin-dependent protein; EGS, ethylene glycolbis (succinimidylsuccinate); MAP, microtubule-associated protein; NGF, nerve growth factor; SDS, sodium dodecyl sulfate; GMPCPP, guanylyl-(α,β)-methylene-diphosphonate.

growth is suggested by two recent experiments where anti-sense oligonucleotides to tau delayed axon extension in regenerating primary cerebellar neurons (Caceres and Kosik, 1990) and where tau protein overexpression induced axon-like processes in Sf9 moth ovary cells (Knops *et al.*, 1991). Recent experiments in PC12 cells, a neuron-like cell line, transfected with sense and anti-sense tau cDNAs also suggest that neurite outgrowth is limited by tau expression because increasing the level of tau stimulated the rate of neurite outgrowth two- to threefold and reduced tau slowed neurite extension threefold (Esmaeli-Azad and Feinstein, personal communication).

Several lines of evidence suggest that phosphorylation may modulate the activity of tau and other MAPs during rearrangements of the microtubule array. Tau is a substrate for two types of kinases, Ca^{2+}/calmodulin-dependent protein (CAM) kinase and MAP2 kinase (also known as myelin basic protein kinase, mitogen-activated protein kinase, or extracellular signal-regulated kinase), both present in PC12 cells (Nose *et al.*, 1985; Landreth *et al.*, 1990; Boulton *et al.*, 1991b; Hilbush and Levine, 1991). CAM kinase treatment induces a mobility shift of tau on sodium dodecyl sulfate (SDS) gels, suggesting a conformational change that could affect tau's interaction with microtubules (Steiner *et al.*, 1990). Treatment of PC12 cells with nerve growth factor (NGF) causes neurite outgrowth and increased levels of MAP2 kinase activity (Tsao *et al.*, 1990; Boulton *et al.*, 1991b). Moreover, MAP2 kinase has been implicated in regulating changes in microtubule dynamics between interphase to mitosis in the early *Xenopus* embryonic cell cycle, and these changes may result from MAP phosphorylation (Gotoh *et al.*, 1991). In brain, tau is highly phosphorylated (Lindwall and Cole, 1984b; Butler and Shelanski, 1986), and tau is readily phosphorylated in vitro by a MAP2 kinase purified from porcine brain (Drewes *et al.*, 1992). Dephosphorylation of bovine brain tau by phosphatase treatment increases its activity in assays measuring the assembly of bulk polymer from purified tubulin (Lindwall and Cole, 1984a). From these bulk assays, we do not know how tau phosphorylation modulates its activity in promoting microtubule assembly: is the effect of phosphorylation simply to decrease tau binding affinity for microtubules or a more specific effect on the ability of tau to alter the dynamic instability properties of microtubule assembly?

To understand how tau modulates the spatial rearrangement of the microtubule array during axon formation, it is necessary to investigate the effects of tau on the dynamic instability properties of tubulin. Because the bulk properties of polymerizing microtubules obscure most of the important properties of the individual polymers, the most direct and unambiguous method for studying tubulin dynamics is to observe individual microtubules in real time. From such observations, one can directly determine the contribution to net assembly of growth, shrinkage, and the frequency of transition between periods of polymerization and depolymerization.

In this study, we find that tau both increases the polymerization rate of individual microtubules and slows their rate of depolymerization. In addition, tau strongly decreases the probability that a growing microtubule will shift from the growing phase to the shrinking phase. We further demonstrate that phosphorylation of tau by MAP2 kinase reduces its activity by lowering the affinity of tau for the microtubule lattice, whereas CAM kinase-mediated phosphorylation of tau has no affect.

MATERIALS AND METHODS

Preparation of Tau and Tubulin

Tubulin was prepared by chromatography on phosphocellulose of three times cycled bovine brain microtubules preparations by the procedure of Weingarten *et al.*, 1975) with modifications described by Mitchison (1984). Tubulin was cycled once more, resuspended to 8 mg/ml, and stored as aliquots at −70°C. Tubulin concentration was determined by Bradford assay using bovine gamma globulin (Bio-Rad, Richmond, CA) as a standard.

Tau was prepared by expression in *Escherichia coli* BL21 cells of the bovine tau clone pBTnde43-12 (derived by changing the initiating met residue of pBT43-12 (Himmler *et al.*, 1989) to an *Nde*I site and inserting the tau sequence into pET3b (Studier *et al.*, 1990). Induced protein was purified by chromatography on phosphocellulose and hydroxyapatite. After dialysis into BRB80 (80 mM K+ piperazine-*N,N'*-bis(2-ethanesulfonic acid), 1 mM ethylene glycol-bis(β-amino-ethyl ether)-*N,N,N',N'*-tetraacetic acid, 1 mM $MgCl_2$, pH 6.8), preparations were concentrated to 2 mg/ml, frozen as aliquots, and stored at −70°C. This tau preparation bound quantitatively to taxol-stabilized microtubules. Tau concentration was determined by absorbance at 279 nm using a value of 0.29 for the extinction coefficient (Cleveland *et al.*, 1977b).

Phosphorylation of Tau by Purified CAM Kinase and MAP2 Kinase

Tau (12 μg) was incubated with 0.1 μg of CAM kinase for 1 h at 4°C with 100 μM ATP in the presence or absence of calmodulin. CAM kinase was kindly provided by Phyllis Hanson and Howard Schulman (Stanford University, Palo Alto, CA). Tau (8 μg) was incubated for 16 h at 30°C with 1 mM ATP, gamma $^{32}PO_4$ labeled ATP, and 2.4 units of MAP2 kinase (1 unit = 2.4 pmol phosphate/min incorporated into myelin basic protein). To control for nonspecific effects on tau during this incubation, hexokinase-agarose (Sigma, St. Louis, MO) and 10 mM glucose were added either before or after MAP2 kinase to deplete ATP and then the immobilized hexokinase was removed from the reaction mixture by centrifugation. MAP2 kinase was purified as previously described (Boulton *et al.*, 1991a).

Preparation of Stabilized Microtubule Seeds for Regrowth Assays

Ethylene glycolbis (succinimidylsuccinate) (EGS)-stabilized microtubule seeds were prepared as previously described (Koshland *et al.*, 1988) with the following modifications. Rhodamine-labeled tubulin (Hyman *et al.*, 1991) was used instead of biotin-labeled tubulin. After preparation, the seeds were diluted to 20% sucrose with BRB80, layered onto a sucrose step gradient (1 ml 40% sucrose, 2 ml 75% sucrose), and centrifuged at 40 000 rpm in a Beckman (Fullerton, CA) SW 50.1

rotor for 40 min at 35°C. The stabilized seeds were collected at the 40–75% interface and stored at room temperature for up to 2 mo.

Microtubule regrowth was performed in BRB80 containing 0.1% b-mercaptoethanol and 5 mM dithiothreitol, prepared as follows. BRB80 was warmed to 60°C and then deaerated for 2 min. After cooling and the addition of reducing agents, the solution was freed from particulate by centrifugation for 15 min at 100 000 × *g* in a TLA100.3 rotor (Beckman). The assembly mixture, prepared from solutions that had been centrifuged for 10 min at 100 000 × *g* in a TLA100 rotor and then transferred to a clean tube and kept on ice, contained tubulin (0–9 μM), tau (0–1 μM), and 0.1% human serum albumin in BRB80 with an anti-fade oxygen scavenging system (50 μg/ml catalase, 100 μg/ml glucose oxidase, 12.5 mM glucose) (Hyman, 1991).

Preparation of the Flow Cell

The microscope slide (Fisher Scientific, Pittsburgh, PA) was cleaned by slowly drawing a piece of lens tissue wetted with 5 μl water across the surface. Coverslips were stored in methanol and dried with lens tissue. The flow chamber was prepared by applying two parallel lines of vacuum grease (Apiezon M, Apiezon Products, London, UK) containing 18-μm beads (1% by weight of SDR 18.2; Duke Scientific, Palo Alto, CA) on the slide and mashing down the coverslip. The flow cell was perfused by applying a solution at one side of the chamber and blotting with a piece of Whatman (Clifton, NJ) 3-mm paper on the opposite side to wick it through. A prewarmed (37°C) flow cell was filled with a 1:100 dilution of rhodamine-labeled EGS-fixed microtubule seeds in BRB80 plus reducing agents. After adsorbing for 2 min, the seeds that had not attached to the glass were flushed out with 40 μl of the assembly mixture (prewarmed for 60 s at 37°C), after which the chamber was sealed with a 1:1:1 mixture of vaseline, lanolin, and beeswax.

Microtubule Dynamics

Microtubule growth was observed using dark-field optics (Olympus [Lake Success, NY] Dark Field Condenser and Nikon [Melville, NY] Plan 50, 0.85 objective). Both condenser and objective were wrapped in silicone tubing connected to a circulating water bath (at ~38°C) so that the temperature of the oil on the slide was constant at 34°C. An image of the rhodamine-labeled seeds was recorded using epifluorescence; microtubule growth was observed by recording a dark-field image every 2–6 s for up to 10 min using a SIT camera (Dage-MTI, Michigan City, IN).

Microtubule Binding Assay

The affinity of tau for taxol-stabilized microtubules was measured as described (Butner and Kirschner, 1991). In this assay, a fixed level of tau is incubated with a range of concentrations of taxol-stabilized microtubules, and the bound tau is separated from the unbound tau by cosedimentation with the microtubules. The dissociation constant, K_d, for tau binding to microtubules is equal to the concentration of microtubules at which half of the tau present cosediments. Tau was detected by western blotting the pellets and supernatants of binding reactions with an affinity purified rabbit antibody to tau, 7A5 (Butner and Kirschner, 1991), horse radish peroxidase-labeled donkey anti-rabbit, and an enhanced chemiluminescence (ECL) detection system (Amersham, Arlington Heights, IL).

RESULTS

Microtubule Assembly With Tubulin Alone

Our goal in these studies was to evaluate the affects of tau on the assembly of microtubules. Previous studies have demonstrated the utility of direct observation for a detailed analysis of microtubule assembly (Summers and Kirschner, 1979; Horio and Hotani, 1986; Walker *et al.*, 1988). Accordingly, we observed by dark-field microscopy the growth of single microtubules in real time. Short rhodamine-labeled microtubules were stabilized and perfused into a perfusion chamber where they adsorbed to the glass surface. Unattached microtubules were washed out, and assembly was initiated by perfusing in unlabeled tubulin. The rhodamine-labeled seeds were visualized by epifluorescence; dark-field microscopy was used to establish the extent and polarity of new assembly. At the low concentrations of tubulin used in this study, usually growth occurred from one end of each seed. Based on previous experiments (Walker *et al.*, 1988), we assumed this to be the plus end. At higher concentrations of tubulin, both ends of the seed grew, and a clear difference in elongation rates between ends was observed. Again, based on previous studies, we identified the faster growing end as the plus end (Allen and Borisy, 1974). In this report, we present an analysis only of the dynamics of the plus ends; we have not included any description of minus ends.

Figure 1 shows sequential dark-field images (representing ~15% of the microscope field) of microtubules assembled in the presence of tau and nucleated from stabilized seeds. The seed was visualized by epifluorescence (bottom). After a period of assembly (287 s), the microtubule switched to a rapid shrinking phase and depolymerization continued back to the stabilized seed (287–317 s) where new assembly began at once (374 s). From such images, we determined the rate of polymerization, the rate of depolymerization, and the frequency at which microtubules switched from growing to shrinking (catastrophe frequency).

Distribution of Growth Rates at a Fixed Concentration of Tubulin

Microtubules polymerized under the same conditions showed a very broad distribution in growth rates, as shown in Figure 2A for four experiments all at 7 μM tubulin. We were interested in whether the breadth of this distribution was due to accumulated errors in measurement or represented real differences in the rate of assembly. Statistical analysis showed that these differences in growth rate were real and therefore must reflect differences in the process of polymerization. Recently, Gildersleeve *et al.* (1992) reported that microtubule regrowth from axonemes occurs at variable rates.

The growth rate was determined by measuring the length from the growing tip to a fixed point on the microtubule seed at two different times (from 5 to 10 min apart). Growth rates were measured from microtubules that grew continuously between measurements as judged by video replays of images recorded at 6 inter-

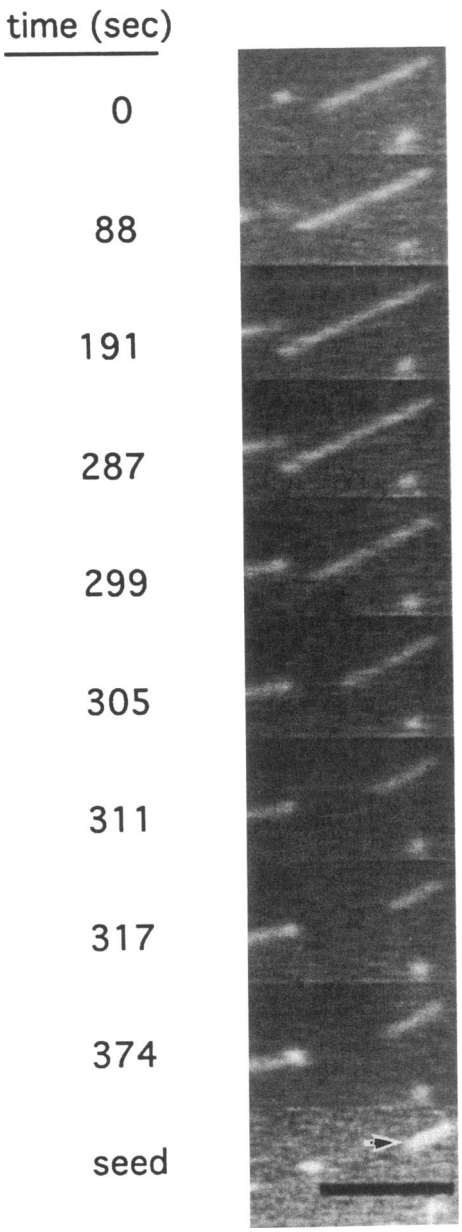

Figure 1. Direct observation of microtubule assembly and disassembly. A short rhodamine-labeled microtubule seed (arrow) stabilized by cross-linking with EGS is viewed by epifluorescence in the last panel (0–374 s). Microtubule assembly in the presence of 1 μM tubulin and 1 μM tau observed by dark-field microscopy. This microtubule grew persistently for 287 s and then abruptly transited to depolymerization (287–317 s), which continued back to the seed where growth resumed (374 s). Scale bar is 5 μm.

vals. We were concerned that in the intervening times between measurements there might have been episodes where growth rate was not uniform. To correct for this, microtubule lengths were measured at every time point where the growing tip was distinct, approximately every 6–21 s. Figure 3 shows the assembly histories of three microtubules in the same microscopic field. One transited to shrinking, whereas the other two grew continuously during observation. At this higher sampling rate (which corresponded to assembly steps of 100–200

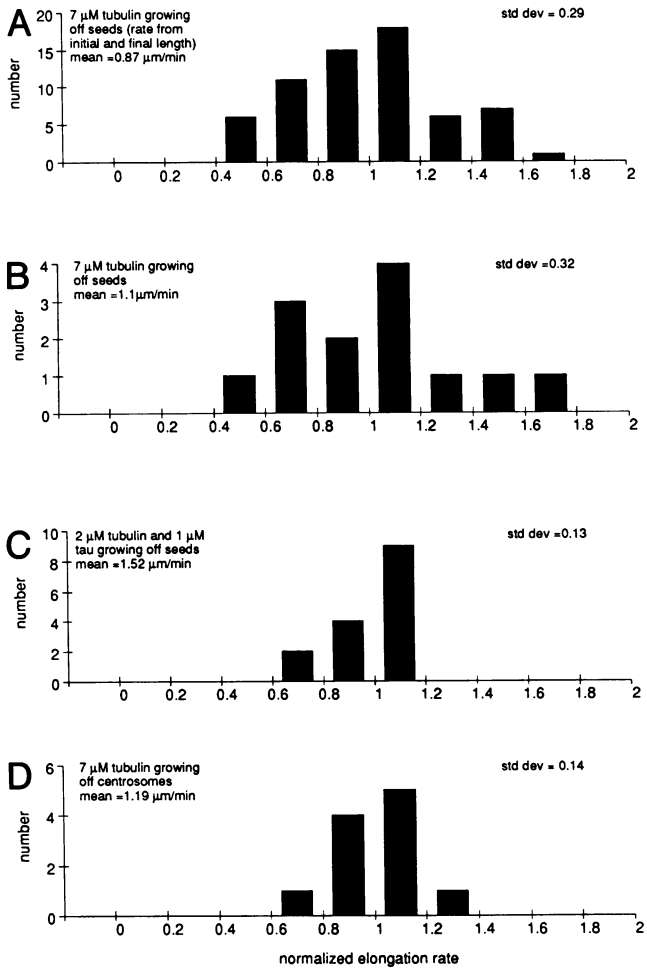

Figure 2. Distributions of microtubule growth rates. These distributions were normalized to a mean of 1 by dividing each data set by its mean growth rate. The means rates ± SD of the means were 0.87 ± 0.26 (A), 1.10 ± 0.36 (B), 1.52 ± 0.21 (C), and 1.19 ± 0.16 μm/min (D). For comparison of these SDs, each distribution was normalized to mean growth rate of 1.0 and the SD of the normalized distribution calculated. These normalized SDs are given in each panel. (A and B) Assembly from seeds in the presence of 7 μM tubulin. (C) Assembly nucleated from seeds with 2 μM tubulin and 1 μM tau. (D) Centrosome-nucleated assembly in the presence of 7 μM tubulin. Two methods of analysis were used to calculate the rate of elongation for individual microtubules. (B, C, and D) Method 1: rates of assembly were calculated from the slope of length vs. time plots with length measured at 6 to 21-s intervals. (A) Method 2: the elongation rate was calculated from the difference in microtubule length between at an initial and final time point. For both methods 1 and 2, images were collected at 6-s intervals and replayed to ensure that no shrinking transits were included during periods where growth rates were determined.

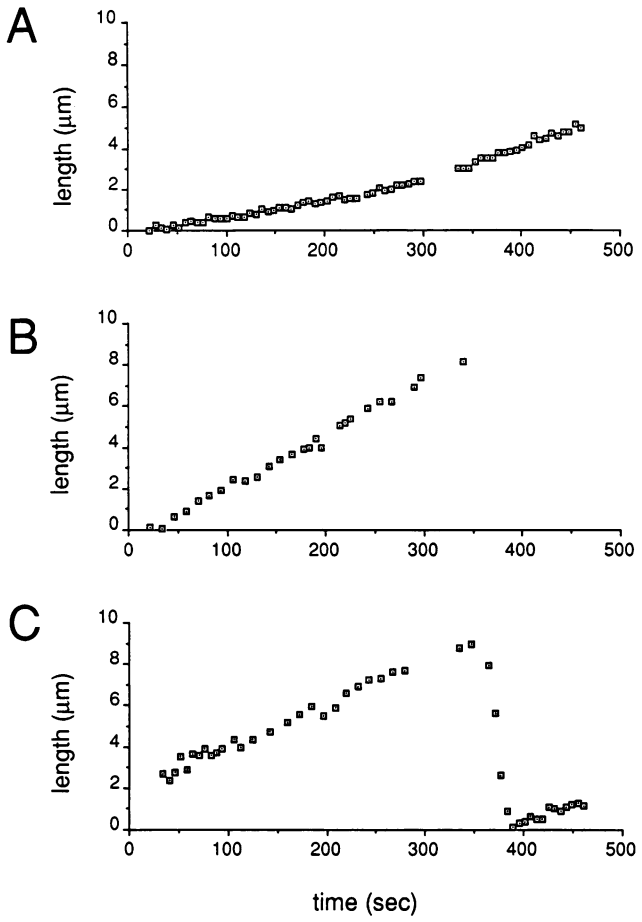

Figure 3. History of assembly for three individual microtubules. Microtubules assembled off stabilized seeds at 7 μM tubulin. Plots represent the distance between the growing tip and the seed during 350–470 s of observation. (A and B) Two microtubules grew continuously during observation at 0.011 μm s^{-1} (A) and 0.026 μm s^{-1} (B). The microtubule in C grew at 0.020 μm s^{-1} for 350 s, when abruptly it entered a shrinking phase and depolymerized back to the seed. Growth resumed at 390 s.

subunits), microtubule assembly from each seed was found to be fairly uniform during the entire time course. Yet as shown, the three assembly rates were very different. Small discontinuities from strictly linear growth were observed in each course of measurement, but these were most likely attributable to errors in measurement and thermal motion of the microtubule. The overall precision in measurement was ±0.1 μm, as determined by repetitive measurement. A larger uncertainty may have been introduced by thermal motion of the microtubule, which could cause bending of long (>5 μm) microtubules; imprecision may have arisen also from rotation of seeds, which were frequently attached at only one end.

During the observations, there were no pauses in growth; at this increased temporal resolution, we also did not observe short periods of shrinking or rapid changes in growth rate. The rate of elongation, calculated from the slope of a history plot after regression analysis, from 13 seeds in a single field of observation, as shown in Figure 2B, gave a broad distribution, with a mean of 1.1 μm/min and a standard deviation of 0.36 μm/min. For comparison of this distribution to other distributions with different mean rates of elongation, we normalized elongation rates to 1.0 and calculated the standard deviation of this normalized distribution. This normalized distribution had a standard deviation of 0.32. This standard deviation was similar to the value of 0.29 found when growth was measured by using only two length measurements. This standard deviation was not due to the large errors in the determination of individual rates, because repeated analysis of a single microtubule resulted in a standard deviation of only 0.02.

We were concerned that these differences in growth rates could be due to microheterogeneities on the coverslip. Gradients in temperature or light intensity could in principal have caused differences in assembly rate. In our microscope, the intensity of illumination is highest in the center of the field and decreases radially. Plots of growth rate as a function of position along the vertical, horizontal, or radial dimensions revealed no correlation between growth rate and position on the coverslip. A second source of heterogeneity in assembly rates could be mismeasurement due to parallax for microtubules that grew obliquely to the surface of the slide. When measured by focusing on beads of calibrated and uniform diameter, we found that our depth of field was <0.5 μm, which would produce a parallax error of 0.4% for the total length of a microtubule 5 μm in length.

These results suggested that the broad distribution in growth rates was due to intrinsic variability in the microtubules themselves rather than errors in measurement. We found that the distribution was much sharper in experiments in the presence of tau protein, as shown in Figure 2C, which has a standard deviation of 0.13. If we compare the breadth of the distributions in Figure 2, A–D, using the rank dispersion test of Siegal and Tukey (Sachs, 1984), we find that both distributions for the growth of pure tubulin off seeds (Figure 2, A and B) have a similar variance, and this variance is statistically different ($P = 0.05$) from the variance of the distribution for growth in the presence of tau. In two experiments using centrosomes and pure tubulin (Figure 2D), we also found a much sharper distribution of growth rates for individual microtubules of 0.14, which was significantly smaller than that for growth of pure tubulin from seeds. The broad distribution of microtubule growth rates must reflect inherent differences in the polymers and not errors in measurement.

Using the seed assay, we compared microtubule growth from pure tubulin with that for tubulin in the presence of 1 μM tau. As shown in Figure 4, tau greatly

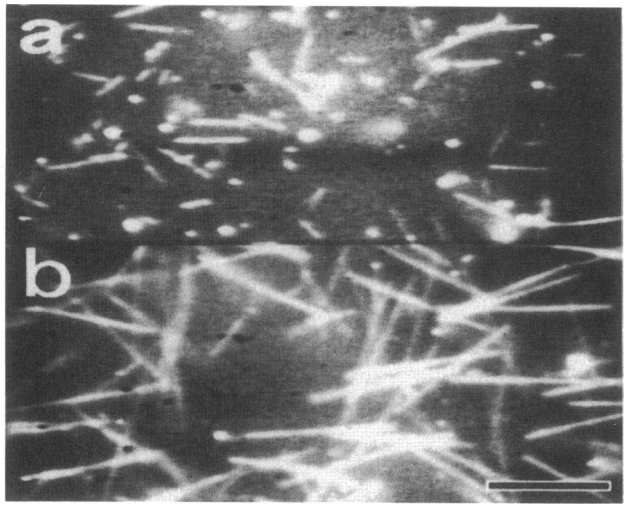

Figure 4. Stimulation of microtubule elongation by tau protein. Dark-field image (a) of microtubule assembly for 300 s from 3 μM tubulin alone and (b) microtubule assembly for 300 s at 3 μM tubulin in the presence of 1 μM tau. Scale bar is 10 μm.

stimulated the elongation of microtubules. The average length of the microtubules grown in the presence of tau (Figure 4b) is ninefold greater than the length of microtubules grown from pure tubulin (Figure 4a). As shown below, this greater length is due to the combined influence of tau on the rate of polymerization, the rate of depolymerization, and the frequency of microtubule catastrophe.

The effect of tau at 1 μM on the rate of microtubule growth is shown in Figure 5A, where it should be remembered that the error bars reflect primarily the dispersion of rates in the population and not inaccuracies in measurement. For tubulin assembly both with and without tau, the growth rate increased linearly with tubulin concentration, and the extrapolated threshold of microtubule assembly (also commonly called the critical concentration) was indistinguishable from zero. This critical concentration was calculated as described below in the DISCUSSION, and the upper limit for its value is 0.05 μM tubulin. Analysis of three experiments showed that at 1 μM, tau-stimulated growth rate 3.2-fold. At a fixed tubulin concentration of 3 μM, tau linearly increased the growth rate (Figure 5B) up to 1 μM tau. Above that concentration, spontaneous nucleation interfered with measurement.

Tau Decreases the Shrinkage Rate

We tested whether the effect of tau on net assembly was due to a decreased rate of microtubule depolymerization. It was not practical to determine the effects of tau on shrinkage rate after the spontaneous transitions to the shrinking phase, because, as shown below, microtubules rarely transit and depolymerize in the presence of tau. Appreciable transitions occurred only at very low concentrations of tubulin, where growth was slow and the average microtubule length was too short to measure accurately. To induce microtubule shrinking, growing microtubules that had been grown from tubulin alone or in the presence or tau were per-

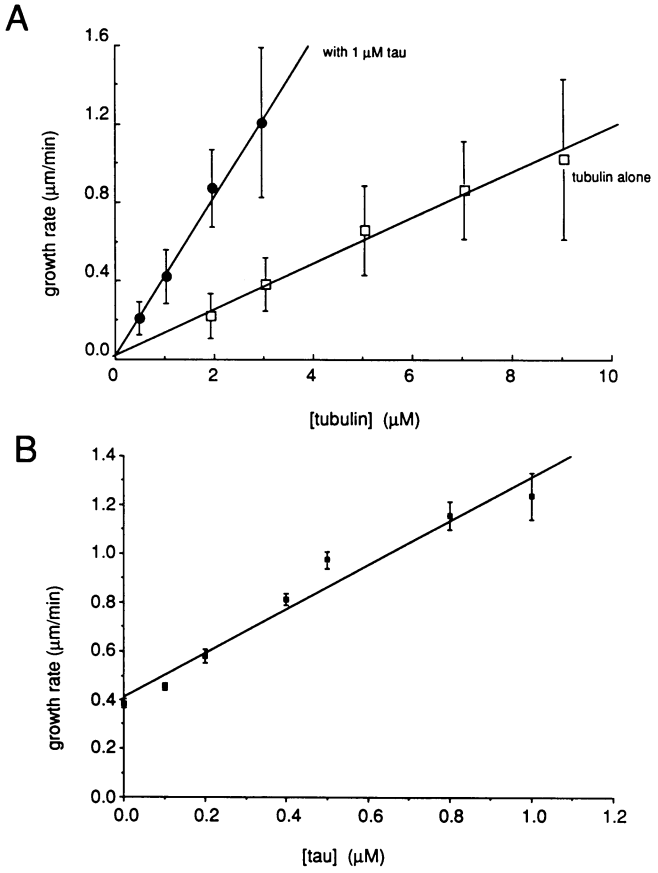

Figure 5. (A) Tau stimulates the growth rate of microtubules at all concentrations of tubulin. Assembly at 2–9 μM tubulin for tubulin alone and at 0.5–3 μM tubulin in the presence of tau. Mean elongation rates (μm/min) at the microtubule plus-end for assembly in the presence of 1 μM tau are indicated by closed circles and mean rates for tubulin alone by open squares. Growth rates were measured from continuously elongating microtubules before any transitions from growth to shrinkage. Linear regression was performed using the complete data set, and the error bars indicate the standard deviation from the mean for the entire data set. The complete data set includes at least three experiments in each of which 20 growing microtubules were measured, except for 2 μM tubulin alone where seeds rarely nucleated assembly and the total number of measured microtubules is 21. (B) Stimulation of microtubule elongation by tau is proportional to tau concentration. Tubulin at 3 μM assembled in the presence of 0–1 μM tau protein. Above 1 μM tau, microtubule assembly was extremely rapid and spontaneous nucleation of microtubules obscured the visualization of polymer assembly off seeds making measurements unreliable. Plot shows mean with the SE (error bars) for three experiments where ≥20 microtubule elongation rates were determined.

fused with buffer alone or with buffer containing tau. All microtubules began to shrink within ~100 s of the start of perfusion. This lag is mostly due to the slow rate of exchange of buffer in the thin chambers (~20 μm thick). Under these conditions, every microtubule in the field entered a shrinking phase. Previous work has shown that microtubules depolymerize at the same rate whether induced by dilution or by spontaneous transit into the depolymerizing phase (Walker *et al.*, 1991). Depolymerization rates also varied but were constant for a given microtubule as shown by the histories in Figure 6, A–C. Variable rates for in vitro microtubule depolymerization have been reported previously (O'Brien *et al.*, 1990; Gildersleeve *et al.*, 1992). Tau at 1 μM decreased the mean rate of depolymerization twofold from 0.18 to 0.088 μm sec^{-1} (Figure 6D).

Growing-to-Shrinking Transition Frequency is Decreased by Tau

An important parameter that affects total bulk assembly is the frequency at which microtubules switch from growing to shrinking, known as the catastrophe frequency. To obtain this frequency, we divided the total number of growing to shrinking transitions at each concentration of tubulin assembly by the total time of microtubule elongation. The results of this analysis are shown in Figure 7A for microtubules of pure tubulin and those polymerized in the presence of 1 μM tau. Transition frequencies are presented as the mean of at least three experiments of typically 20 microtubules. As previously shown for pure tubulin (Walker *et al.*, 1988), the microtubule catastrophe frequency decreased steeply with increasing tubulin concentration. For example, the frequency of transitions (0.0033 s^{-1}) at 5 μM tubulin was fourfold lower than at 2 μM tubulin (0.0133 s^{-1}). Above 5 μM tubulin, transition frequencies appeared independent of tubulin concentration and plateaued at a constant value near 0.0017 s^{-1}.

In the presence of tau, the transition frequency was also highly dependent on tubulin concentration. However, tau markedly suppressed transitions at all levels of tubulin. At 3 μM tubulin, the presence of 1 μM tau lowered the transition frequency ≥50-fold (no shrinking microtubules were ever observed) from 0.0083 s^{-1} to <0.0002 s^{-1}. Only at very low tubulin concentrations (≤1 μM tubulin) were transitions observed in the presence of 1 μM tau.

For the assembly of pure tubulin, both the transition frequency and the elongation rate were found to be highly dependent on tubulin concentration, with high tubulin levels leading to faster growth and infrequent catastrophes. Because microtubules that grow faster shrink less often and tau protein stimulated the rate of elongation, we were interested in whether the decreased transition frequency was a direct result of the increasing

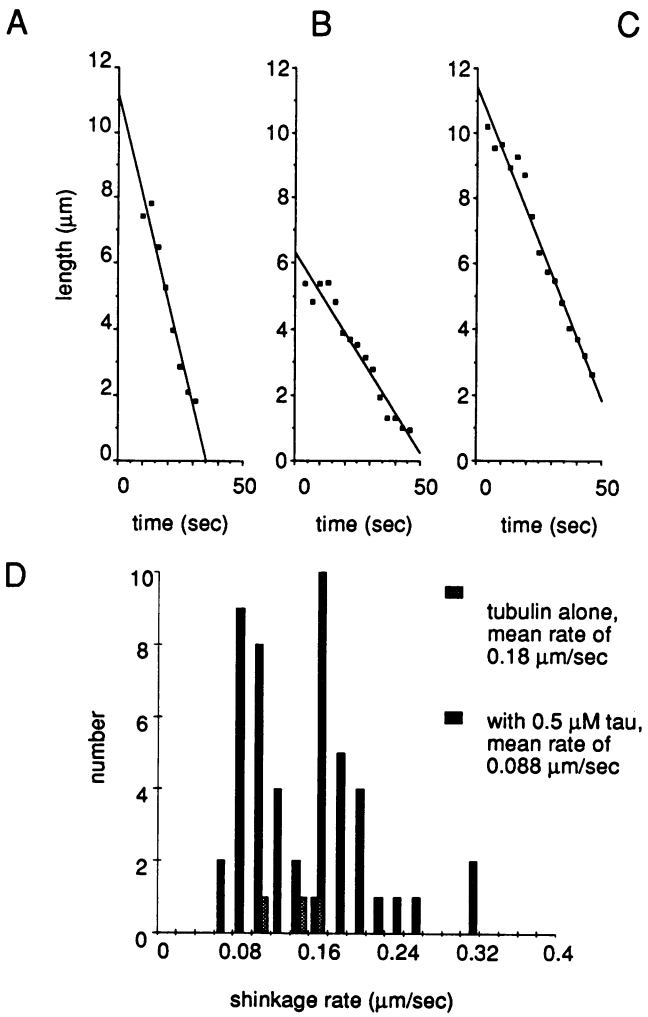

Figure 6. (A–C) History of depolymerization induced by dilution. Microtubules were assembled off seeds at 7 μM tubulin until ~10 μm in length. Perfusion with buffer alone induced rapid disassembly. The microtubule length was measured from images acquired at 2-s intervals and rate of shrinkage calculated from the slope of length vs. time plots. The individual microtubules shown here shrank at 0.32 (A), 0.12 (B), and 0.19 μm/s (C). (D) Tau protein slowed the rate of microtubule depolymerization. Microtubules assembled from tubulin alone (7 μM) or from tubulin (3 μM) in the presence of tau (0.5 μM) all entered shrinking phases on perfusion with buffer alone or buffer containing tau. Filled bars represent the number of microtubules depolymerizing within the indicated range of depolymerization rates (μm/min) for tau-coated microtubules, and stippled bars indicate the rates of disassembly for microtubules assembled from tubulin alone.

growth rate, a prediction of the simplest GTP cap models that attempt to explain the dynamic instability of tubulin assembly (Kirschner and Mitchison, 1986). In Figure 7B, we plotted the transition frequency against the rate of elongation. The disparity in the plots for tubulin and tau demonstrates that the inhibition of catastrophe rate by tau cannot be solely attributed to increased growth rate.

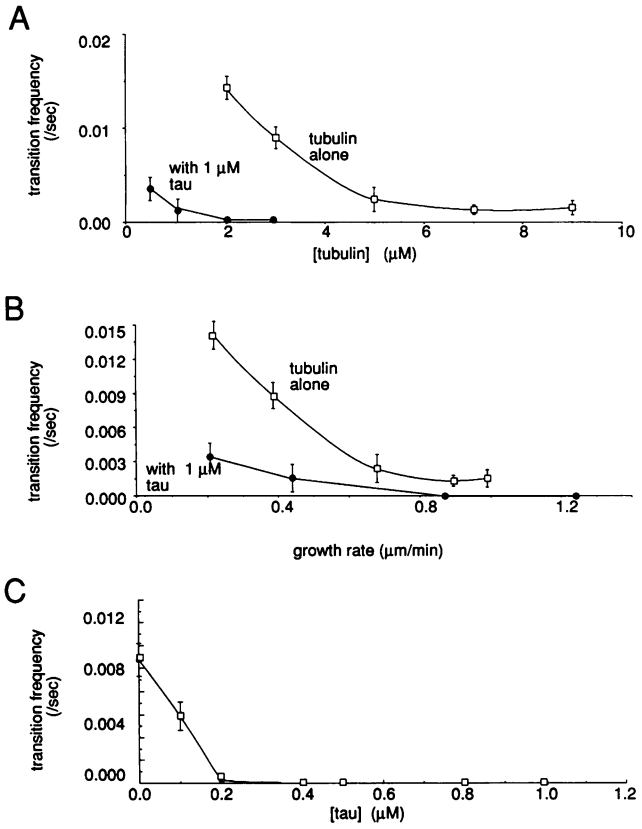

Figure 7. (A) Tau strongly suppressed the frequency at which growing microtubules transit to shrinking. Transition frequency was calculated from the total number of transitions divided by the total time of growth. Assembly behavior was observed at 2–9 μM tubulin for tubulin alone and at 0.5–3 μM tubulin in the presence of 1 μM tau. Open squares represent the mean transition frequency (s^{-1}) with the SE (error bars) for three experiments where ≥20 microtubules were observed during assembly from tubulin alone. Closed circles indicate the transition frequency in the presence of tau. (B) Transition frequency is plotted as a function of growth rate for tubulin alone (2–9 μM) and tubulin (0.5–3 μM) in the presence of tau (1 μM). At equivalent rates of growth, microtubules in the presence of tau (●) exhibit suppressed catastrophe frequencies when compared with microtubules assembly from pure tubulin (□). (C) Tau inhibition of transitions from growth to shrinkage is strongly dependent on the concentration of tau. Tubulin assembled at 3 μM in the presence of variable levels of tau. Values represent the mean and the SE (error bars) for three experiments where 20 microtubules were observed.

Transition Frequency Depends on Tau Concentration

In Figure 7C, microtubule assembly was observed at 3 μM tubulin in the presence of varied amounts of tau (0–1 μM). The effect of tau on transition frequency was found to follow the binding for tau to microtubules, with a half-maximal effect on transition frequency at 0.1 μM, equal to the dissociation constant found for tau binding to taxol-stabilized microtubules (Butner and Kirschner, 1991). Above 0.3 μM tau, there is essentially no evidence for dynamic instability (transition frequency $< 0.0002\ s^{-1}$).

Effect of Phosphorylation of Tau by MAP2 Kinase and CAM Kinase on Microtubule Dynamics

Tau can be phosphorylated by purified MAP2 kinase to a stoichiometry of 3–4 mol PO_4/mol tau, as determined by radioactive labeling. This stoichiometry of phosphorylation by MAP2 kinase caused a shift in migration on SDS-polyacrylamide gel electrophoresis (Figure 8). Control solutions depleted of ATP by the addition of glucose and hexokinase before incubation with MAP2 kinase showed no incorporation of ^{32}P and no mobility shift (Figure 8). Phosphorylation of tau by MAP2 kinase completely abolished the twofold effect of tau on microtubule assembly rate, measured at a concentration of tau of 0.5 μM (Table 1). Surprisingly,

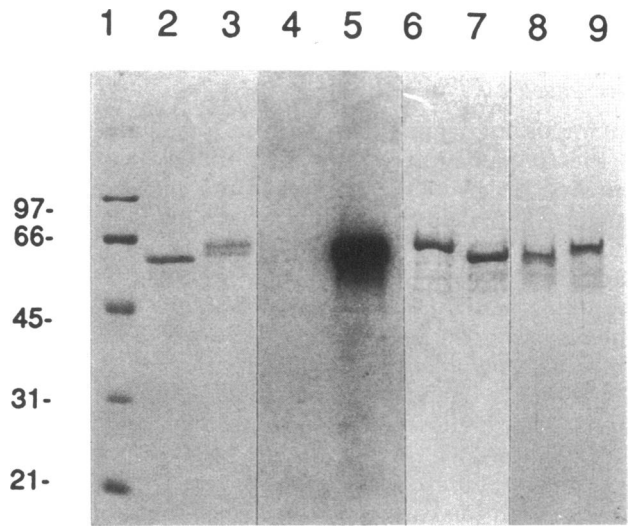

Figure 8. Phosphorylation of tau by purified MAP2 kinase and CAM kinase. Lanes 2–5 show phosphorylation of tau by MAP2 kinase. Tau (8 μg) was incubated for 16 h at 30°C with 1 mM ATP, gamma $^{32}PO_4$ labeled ATP, and MAP2 kinase (see MATERIALS AND METHODS). Hexokinase-agarose was added either before (lanes 2 and 4) or after (lanes 3 and 5) MAP2 kinase to deplete ATP and then removed from the reaction mixture by centrifugation. (Lane 1) Molecular weight standards. (Lanes 2 and 3) Preparations stained with Coomassie Blue after electrophoresis on 10% SDS gels. MAP2 kinase treatment of tau produced a shift in apparent molecular weight. (Lanes 4 and 5) Autoradiograph of lanes 2 and 3 shows that hexokinase depletion of ATP prevents $^{32}PO_4$ incorporation only if hexokinase is added before MAP2 kinase. Lanes 6–9 show phosphorylation of tau by CAM kinase. Tau (12 μg) was incubated with 0.1 μg of CAM kinase for 1 h at 4°C with 100 μM ATP in the presence (lanes 6 and 9) or absence (lanes 7 and 8) of calmodulin, an essential activator of CAM kinase activity. (Lanes 6 and 7) Coomassie-stained preparations after electrophoresis on 10% SDS gels. CAM kinase treatment of tau caused a shift in apparent molecular weight of tau. (Lanes 8 and 9) After incubation with tubulin for 15 min at 37°C, samples were transferred to nitrocellulose and probed with 1:200 dilution of 7A5, an affinity-purified rabbit antibody to the amino terminus of bovine tau protein, followed by an alkaline phosphatase-labeled secondary goat anti-rabbit (Bio-Rad). CAM kinase treatment of tau caused a shift in apparent molecular weight that remained after incubation with the tubulin assembly mixture.

Table 1. Effect of tau phosphorylation on microtubule assembly[a]

	Tau (μM)	Growth rate (μm/min)	Catastrophe rate (/s) × 1000	Microtubule affinity K_d (μM)	n
Tubulin alone (3 μM)	0.0	0.38 ± 0.02	9.0 ± 1.2	NA	7
Native tau	0.5	0.97 ± 0.14	0.0	0.1	4
	0.2	0.58 ± 0.09	0.3 ± 0.2		3
	0.1	0.46 ± 0.04	4.9 ± 1.0		3
CAM kinase-treated tau	0.5	0.90	0.1	ND	1
	0.2	0.53	0.0		1
	0.1	0.41 ± 0.04	1.2 ± 0.5		3
CAM kinase-treated tau (no calmodulin control)	0.5	1.00	0.0	ND	1
	0.1	0.42	1.0		2
MAP2 kinase-treated tau	0.5	0.34 ± 0.02	0.6 ± 0.3	1	3
	4.0	0.83	0.0		2
MAP2 kinase-treated tau (no ATP control)	0.5	0.73	0.0	ND	3

[a] Microtubule polymerization was observed at 3 μM tubulin with various levels of native and phosphorylated tau. Growth rates represent the mean ± SD for the indicated number (n) of experiments, where in each experiment typically 20 microtubules were measured. Catastrophe rates represent the mean ± SE. NA, not applicable; ND, not determined.

phosphorylated tau retained a strong but diminished ability to suppress transitions to shrinking, reducing the catastrophe rate ≥ 10-fold from 0.009 s^{-1} for tubulin alone to 0.0006 s^{-1} with phosphorylated tau. Compared with native tau, where transitions to shrinking were never observed at these levels of tubulin and tau, phosphorylation was inhibitory because many transitions were observed. This loss of activity could have been due to either a loss of binding affinity or to a change in the assembly-promoting activity of tau. If phosphorylation lowered the binding affinity, then activity should be restored by assaying higher concentrations of phosphorylated tau. Indeed, when assayed at 4 μM, phosphorylated tau increased microtubule growth rate and completely suppressed transitions (Table 1). To measure the loss of binding directly, we determined the K_d for phosphorylated and native tau by cosedimentation with taxol-stabilized microtubules (Butner and Kirschner, 1991). The K_d was found to be 10-fold higher for phosphorylated tau (K_d = 1 μM) compared with native tau (K_d = 0.1 μM).

Because previous work had shown that the phosphorylation of a single site on tau by CAM kinase induces a mobility shift on SDS gels (Steiner *et al.*, 1990), we examined the effects of phosphorylation by CAM kinase on the activity of tau. Tau was phosphorylated by incubation with purified CAM kinase. The stoichiometry of phosphorylation was judged by the mobility shift on SDS gels. Control solutions of tau incubated with kinase lacking calmodulin, an essential activator of CAM kinase activity, showed no such shift in tau mobility.

Fully phosphorylated tau and control solutions of tau were added to assembly reactions containing 3 μM tubulin, and the effects on the dynamic instability of tubulin assembly were followed. In contrast to MAP2 kinase, phosphorylation of tau protein by CAM kinase had no effect on the promotion of tubulin assembly by tau. Both the increase in growth rate and the decrease in transition frequency were unchanged at 0.5 μM phosphorylated tau (Table 1). We were concerned that contaminating phosphatase present in the tubulin preparation may have removed the phosphate added by CAM kinase. To ensure that tau remained phosphorylated during the assembly reaction, samples before and after incubation with tubulin were analyzed by western blotting to detect the shift in migration of tau that characterizes tau phosphorylation with CAM kinase. After a standard assembly reaction for 15 min, the CAM kinase-treated tau showed no evidence of dephosphorylation (Figure 8).

DISCUSSION

In this article, we have examined the mechanism by which tau modulates the assembly of tubulin. It is well documented from bulk measurements that tau increases the rate, length, and extent of microtubule growth (Cleveland *et al.*, 1977a; Bre and Karsenti, 1990). Previous studies could not discriminate among the relative contributions of changes in polymerization rate, depolymerization rate, and the frequency of transitions between growth and shrinkage to this increase in growth, because tubulin assembly was assayed either by monitoring changes in bulk polymer levels or by measuring changes in the average length of fixed microtubules. In our experiments, we observed the growth of single microtubules in real time and we could con-

sequently demonstrate that the effects of tau at the plus end are the aggregate of three processes: an increase in the rate of elongation, a decrease in the transit to the shrinking phase, and a decrease in the rate of depolymerization.

A Direct Effect of Tau on the on Rate of Assembly

It generally has been thought that MAPs stabilize microtubules by decreasing the off-rate of tubulin (Murphy *et al.*, 1977). In many cases, the on-rate for polymer formation is assumed to be at the diffusion controlled rate, and hence it is difficult to imagine how the binding of any protein to the lattice can affect that rate. The results here, however, suggest that tau has a significant effect on the on-rate, and any effect on the off-rate makes a negligible contribution to the net rate of assembly.

To explain the basis for these conclusions, we first consider the complexities of dynamic instability. Microtubules exist in two phases, growing or shrinking, with very different kinetic properties (Mitchison and Kirschner, 1984). In each phase they have a rate of tubulin subunit addition and a rate of subunit loss. Each tubulin subunit hydrolyzes a single bound GTP to GDP shortly after assembly of the subunit onto the growing microtubule, and it is generally thought that the shrinking phase is the characteristic phase of GDP-tubulin ends, whereas the growing phase is characteristic of GTP-tubulin ends (Hill and Carlier, 1983). The off-rate in the shrinking phase is much larger than the on-rate and is easy to measure directly by infinite dilution because microtubules rapidly enter the shrinking phase on infinite dilution. In contrast, the off-rate in the growing phase is small compared with the on-rate and cannot be directly measured. Because the aggregate growth rate (the net rate of subunit addition and loss) in the growing phase is linear, it is assumed that the off-rate for the growing phase can be calculated by an extrapolation of the aggregate rate to zero tubulin concentration.

We have found that tau promoted a net increase in subunit addition to the plus end of the microtubule during the growing phase. In principle, this could be due to either an increase in the on-rate or a decrease in the off-rate. Subunit addition is proportional to tubulin concentration, whereas subunit loss is independent. In terms of the rate constants (k_{on}^{grow}) and (k_{off}^{grow}) for tubulin subunit addition and loss, the net rate of microtubule assembly for growing microtubules is given by:

$$\text{net growth rate} = k_{on}^{grow}\,(\text{tubulin concentration}) - k_{off}^{grow}$$

k_{off}^{grow} is the extrapolated rate at zero tubulin (the y intercept of Figure 5A). In this study, we find that this extrapolated rate of subunit loss (k_{off}^{grow}) is very small. Using statistical tests, we can estimate the largest value that k_{off}^{grow} could have (with 95% confidence), and this value is extremely low (0.1 s^{-1}), corresponding to a depolymerization rate of 0.005 μm min^{-1}. The concentration of tubulin where the on-rate equals the off-rate, k_{off}^{grow}, is commonly called the critical concentration for assembly and is equal to the x intercept in Figure 5A. Using k_{off}^{grow} to calculate the critical concentration, a very low value (0.05 μM) is obtained for the lower limit of tubulin concentration that supports microtubule assembly. This low critical concentration was similar to a previous study of microtubule assembly (Mitchison, 1984) that measured microtubule growth from stable nucleating centers at fixed time points and found a critical concentration of 0.1 μM but differed from a more recent study (Walker *et al.*, 1988) that measured microtubule assembly using real time observation of individual microtubules. In this latter study, the critical concentration of plus end growth was 5 μM tubulin, and k_{off}^{grow} was found to be 44 s^{-1}. We cannot be certain about the reason for this discrepancy, but several differences exist in the Walker *et al.* experiments, including the preparation of tubulin, the presence of serum albumin as a carrier in the assembly assay, and the use of different nucleating sites. Assembly with guanylyl-(α,β)-methylene-diphosphonate (GMPCPP), a nonhydrolyzable analogue of GTP, allows another and perhaps more direct measure of the off-rate in the growing phase, because the shrinking phase of microtubule assembly is never observed when tubulin assembles in its presence. In support of our low extrapolated value for k_{off}^{grow} of 0.1 s^{-1}, the same value of 0.1 s^{-1} was also found for the off-rate of GMPCPP tubulin subunits (Hyman *et al.*, 1992).

To estimate the contribution of tau to the on-rate and off-rate, we first considered the measured effects of tau on assembly. At 3 μM tubulin, tau increases the on-rate from 9 to 33 subunits s^{-1}. Because we found a very low off-rate (0.1 s^{-1}), tau cannot appreciably increase the rate of elongation by suppressing the loss of tubulin monomers from the growing tip. (The maximum on-rate that could be obtained if tau reduced the off-rate to zero would be 9.1 s^{-1}, as compared with the measured value of 33 s^{-1}.)

How could tau increase the on-rate? The rate of subunit incorporation at the growing end of the microtubule must only be a fraction of the total collisions of subunits at the microtubule end. Tau could increase the fraction of productive collisions by increasing the target area for assembly, by blocking electrostatic repulsion at the growing tip, or by changing the conformation of the terminal tubulin subunit to favor addition of an incoming subunit. Tau could increase the collision target by binding near the microtubule end, such that a portion of the diffuse microtubule binding region on tau is not

bound to the microtubule and available for binding to a tubulin subunit. Tau could decrease the electrostatic repulsion encountered by an incoming tubulin subunit at the end of a growing microtubule because tau is very basic and tubulin quite acidic. Tau could affect the rate of polymerization by changing the nature of the tubulin subunit. Tau has been shown previously to interact with tubulin in the unpolymerized state to form various large oligomers of tubulin (Cleveland *et al.*, 1977a). In general, oligomerization would not be expected to increase the rate of polymerization, because for any increase in the number of subunits added per assembly event by virtue of oligomerization, there must be a corresponding decrease in the concentration of oligomer over monomer. Finally, tau could affect the rate of polymerization by stabilizing a form of tubulin that would make more productive collisions with the microtubule lattice or a form on the lattice that would make more productive collisions with the incoming subunits. In this view, tubulin might exist in an equilibrium between an assembly-competent and an assembly-incompetent form, and tau might bind to the competent form and increase its representation.

Given the very low measured value of the critical concentration, it may seem surprising that we observed no polymerization at low monomer levels. In the absence of tau, we failed to observe growth off seeds below 2 μM tubulin, which is well above the extrapolated critical concentration for microtubule assembly (0.05 μM). This failure was most likely due to the steeply increasing rate of transitions to a shrinking phase (catastrophe events) observed with decreasing tubulin concentrations rather than an inherent inability of tubulin to grow at low concentrations. Assembly in the presence of GMPCPP supports this view because catastrophe events are never observed during polymerization using this nonhydrolyzable analogue of GTP, and microtubule polymerization is observed at much lower tubulin concentrations (0.25 μM) (Hyman *et al.*, 1992). Likewise, in the presence of tau, which greatly suppresses catastrophes, the lower limit of growth was decreased to 0.5 μM tubulin.

Catastrophe Rate is not Simply a Function of Growth Rate

In the first formulation of dynamic instability, the growing phase was attributed to a GTP cap that disappeared stochastically (Mitchison and Kirschner, 1984). The size of the GTP cap would be expected to be larger at faster growth rates, and this explanation was consistent with the lower catastrophe rate at high rates of growth. More recent experiments have failed to find a large stable GTP cap, even at rapid growth rates (O'Brien *et al.*, 1987; Schlistra *et al.*, 1987; Stewart *et al.*, 1990; Walker *et al.*, 1991). The lower rate of catastrophe at the slower growing minus end also suggested that there was not a strict correspondence between growth rate and catastrophe rate (Walker *et al.*, 1988). The effect of tau on suppressing the rate of microtubule catastrophe again raises the question of whether growth rate and suppression of catastrophe are distinct. Tau both increases the growth rate and decreases the catastrophe rate (growth to shrinking transition). However, at low tau concentrations, tau exhibits a much stronger transition frequency suppression than augmentation of microtubule growth rate. For example, at 3 μM tubulin, tau at a concentration of 0.2 μM lowers the catastrophe rate 30-fold from 0.0083 to 0.0003 s^{-1}. This concentration of tau increased the growth rate only ~1.5-fold to equal the growth rate of pure tubulin at 4.5 μM tubulin. At that concentration of pure tubulin, the transition frequency is 0.0037 s^{-1} or still 12 times greater than that for 0.2 μM tau and 3 μM tubulin. Furthermore, comparing the growth rates of pure tubulin to the growth rates of tubulin plus 1 μM tau in Figure 7B, it is clear at any given growth rate the catastrophe rates for tau are always much less than for pure tubulin. Thus, in addition to stimulating polymerization, tau also has an additional effect of reducing the catastrophe rate. This dissociation of microtubule growth rate and transition frequency is also observed during assembly of tubulin in the presence Mg^{2+} (O'Brien *et al.*, 1990).

Treatment of tau with MAP2 kinase provides another instance where the effect of tau on growth rate and transition frequency are separable. When assayed at a level where native tau doubles the growth rate (0.5 μM), MAP2 kinase-treated tau had no effect. Despite this complete inhibition of tau's effect on growth rate, phosphorylated tau retained a substantial activity to suppress transitions, although this activity was reduced compared with native tau.

This suppression of transitions is not likely to have been due to a capping of microtubule ends by tau because dilution of tubulin monomer induced a rapid transition to shrinking even in the presence of high concentrations of tau. Rather than interacting specifically with the tip, tau must bind to the sides of the microtubule lattice and provide lateral stability near the tip, which decreases the rate of catastrophes. Tau has effects on microtubule shrinkage. As shown in Figure 6D, when saturated with tau protein, microtubules shrink more slowly. The mean rate of shrinkage decreased nearly twofold from 490 to 270 s^{-1}. Recent cryoelectron microscopy images of shrinking microtubules suggest that disassembly occurs by the peeling away of long protofilaments of tubulin rather than loss of individual subunits (Mandelkow and Mandelkow, 1991). In this case, tau stabilization could involve inhibition of protofilament peeling by increasing lateral interactions between protofilaments. Alternatively, tau may have some specific effects on the poorly understood GTP

cap. Tau might act to prevent transitions to shrinking by preferentially slowing the loss of GTP subunits or by inhibiting GTP hydrolysis. We would expect tau to increase rescue by decreasing the rate of shrinkage, but the low frequency of catastrophe in the presence of tau made it impossible to test this prediction.

Nonuniformity of Microtubule Growth Rates

Using pure tubulin, we observed a broad distribution of microtubule growth rates from seeds, under identical conditions. Variable rates of growth are also found during microtubule regrowth from axonemes (Gildersleeve *et al.*, 1992). These differences in rate are real and are far beyond what might be expected due to stochastic fluctuation in the number of subunits that assemble. The persistence of the growth rate differences suggests that they arose at the time of nucleation and point to the seeds as the source of a heterogeneity that is propagated during elongation. One possible heterogeneity in the microtubule lattice is protofilament number. Indeed, differences in protofilament number have been found in microtubules. Microtubules assembled in vitro off centrosomes had different numbers of protofilaments than those nucleated spontaneously under the same conditions (Evans *et al.*, 1985). In this case, centrosomal growth restricted protofilament number to 13, whereas spontaneous polymerization produced microtubules with almost exclusively 14 protofilaments. More recent analysis of protofilament number from electron micrographs of microtubules suggests that protofilament number can vary from 12 to 16 and that protofilament number can vary within a single microtubule (Chretien *et al.*, 1992). The touch receptor neurons in *Caenorhabditis elegans* provide another example of differences in protofilament number with a class of microtubules in these cells showing 15 protofilaments, where the normal number for that species is 11 (Savage *et al.*, 1989).

We found that the distribution of growth rates off centrosomes was more restricted (more uniform) than growth from seeds. This uniformity may reflect a uniformity in protofilament number. We also found that microtubules grown from seeds in the presence of tau exhibited a more uniform distribution of growth rates compared with microtubules grown from pure tubulin. In this way, growth in the presence of tau was similar to growth off centrosomes. This would lead to the prediction that microtubules grown in the presence of tau might exhibit a restricted protofilament number and that tau may stabilize the 13 protofilament form. Perhaps a MAP with tau-like properties is present on the centrosome and is responsible for the uniformity of growth and the stimulation of nucleation at low tubulin concentrations.

Tau Phosphorylation Modulates Interaction With Microtubules

The phosphorylation of tau has been linked in several ways to changes in microtubule assembly. Treatments of PC12 cells that stimulate neurite outgrowth increase the activity of both MAP2 kinase and CAM kinase (Tsao *et al.*, 1990; Hilbush and Levine, 1991), both of which may act on tau protein. Tau protein is also induced during neurite outgrowth of PC12 cells stimulated by NGF treatment (Drubin *et al.*, 1985). We found that both enzymes phosphorylated tau stoichiometrically. CAM kinase incorporated 1 mol PO_4/mol and MAP2 kinase added 3–4 mol PO_4/mol of tau protein. The single site of tau phosphorylation by CAM kinase is outside the microtubule-binding domain at serine-405 (Steiner *et al.*, 1990). Recently, Drewes *et al.* (1992) reported that purified MAP2 kinase from porcine brain can incorporate 14–16 phosphates per tau molecule, suggesting that nearly all of the possible consensus sites (S/TP) (Haycock *et al.*, 1992) in tau are recognized by MAP2 kinase. We found that tau phosphorylated by CAM kinase was unchanged in its capacity to influence microtubule assembly when compared with native tau. Treatment of tau with MAP2 kinase, in contrast, leads to a marked loss of microtubule assembly-promoting activity due to a 10-fold loss of microtubule-binding affinity. This change in microtubule affinity suggests that phosphorylation of tau might control tau binding to microtubules in neurons, thereby affecting the growth and stability of the microtubule array.

Role of Tau In Vivo

We have examined the effects of tau on microtubule assembly in vitro. The results of these experiments suggest that tau suppresses microtubule dynamics without abolishing dynamics. At low levels (0.1–0.2 μM), tau dramatically reduces the catastrophe frequency of microtubules, and at higher concentrations it increases the rate of polymerization of growing microtubules and decreases the rate of depolymerization of shrinking microtubules. These properties suggest that tau provides a strong but limited stability to microtubules. This stabilization is rapidly reversible by phosphorylation by MAP2 kinase. Phosphorylation of tau by MAP2 kinase reduces the ability of tau to stabilize microtubules by decreasing the affinity of tau for microtubules ~10-fold from 0.1 μM in the absence of phosphorylation to 1 μM after phosphorylation by MAP2 kinase. MAP2 kinases have been identified as important intermediates in kinase cascades activated after stimulation of transmembrane receptors, such as the insulin, NGF, and fibroblast growth factor receptors (Cobb *et al.*, 1991), and signal to downstream targets. These kinases are highly expressed in neurons (Boulton *et al.*, 1991b). The concentration of tau in neurites is ~1 μM (Drubin *et al.*,

1985), demonstrating that the effects that we have measured in vitro are likely to reflect a role for tau in stabilizing microtubules in vivo and these effects could easily be modulated by phosphorylation.

The abnormal properties of tau in Alzheimer's disease in forming paired helical filaments (also known as neurofibrillary tangles) may be related to the effect of phosphorylation on the affinity of tau for microtubules because tau exhibits an abnormal state of phosphorylation when present in these filaments (Grundke-Iqbal *et al.*, 1986; Ueda *et al.*, 1990; Lichtenberg-Kraag *et al.*, 1992). It is difficult to know whether accumulation of tau or phosphorylation of tau are primary events. However, it is possible that phosphorylation of tau could cause microtubule destabilization, generating a pool of unassembled tubulin and tau. The pool of unassembled tau may in turn be subject to further modification (e.g., ubiquitination or phosphorylation), leading to the abnormal assembly of tau into the characteristic paired helical filaments.

ACKNOWLEDGMENTS

We gratefully acknowledge Phyllis Hanson and Howard Schulman for providing purified CAM kinase. We thank Karen Butner, Tim Mitchison, Andrew Murray, Ken Sawin, and Elly Tanaka for suggestions and critical comments on the manuscript. Moss Prescott and Arthur Conner developed image analysis software that greatly aided this study. Friends of Microtubules (at UCSF) provided continuous encouragement during the course of these experiments. A.A.H. is a Lucille P. Markey scholar, and this work was funded in part by a grant from the Lucille P. Markey Foundation. This work received general support from the National Institute of General Medical Sciences (M.W.K.).

REFERENCES

Allen, C., and Borisy, G.G. (1974). Structural polarity and directional growth of microtubules of *Chlamydomonas flagella*. J. Mol. Biol. *90*, 381–402.

Black, M.M., Aletta, J.M., and Greene, L.A. (1986). Regulation of microtubule composition and stability during nerve growth factor-promoted neurite outgrowth. J. Cell Biol. *103*, 545–557.

Boulton, T.G., Gregory, J.S., and Cobb, M.H. (1991a). Purification and properties of extracellular signal-regulated kinase 1, an insulin-stimulated microtubule-associated protein 2 kinase. Biochemistry *30*, 278–286.

Boulton, T.G., Nye, S.H., Robbins, D.J., Ip, N.Y., Radziejewska, E., Morgenbesser, S.D., DePinho, R.A., Panayotatos, N., Cobb, M.H., and Yancopoulos, G.D. (1991b). ERKs: a family of protein-serine/threonine kinases that are activated and tyrosine phosphorylated in response to insulin and NGF. Cell *65*, 663–675.

Bre, M.H., and Karsenti, E. (1990). Effects of brain microtubule-associated proteins on microtubule dynamics and the nucleating activity of centrosomes. Cell Motil. Cytoskeleton *15*, 88–98.

Butler, M., and Shelanski, M.L. (1986). Microheterogeneity of microtubule-associated tau proteins is due to differences in phosphorylation. J. Neurochem. *47*, 1517–1522.

Butner, K.A., and Kirschner, M.W. (1991). Tau protein binds to microtubules through a flexible array of distributed weak sites. J. Cell Biol. *115*, 717–730.

Caceres, A., and Kosik, K.S. (1990). Inhibition of neurite polarity by tau antisense oligonucleotides in primary cerebellar Neurons. Nature. *343*, 461–463.

Chretien, D., Metoz, F., Verde, F., Karsenti, E., and Wade, R.H. (1992). Lattice defects in microtubules: protofilament numbers vary within individual microtubules. J. Cell Biol. *117*, 1031–1040.

Cleveland, D.W., Hwo, S.-Y., and Kirschner, M.W. (1977a). Purification of tau, a microtubule-associated protein that induces assembly of microtubules from purified tubulin. J. Mol. Biol. *116*, 207–225.

Cleveland, D.W., Hwo, S.-Y., and Kirschner, M.W. (1977b). Physical and chemical properties of purified tau factor and the role of tau in microtubule assembly. J. Mol. Biol. *116*, 227–247.

Cobb, M.H., Boulton, T.G., and Robbins, D.J. (1991). Extracellular signal-regulated kinases: ERKs in progress. Cell Regul. *2*, 965–978.

Daniels, M.P. (1972). Colchicine inhibition of nerve fiber formation in vitro. J. Cell Biol. *53*, 164–176.

Drewes, G., Lichtenberg-kraag, B., Döring, F., Mandelkow, E.-M., Biernat, J., Goris, J., Dorée, M., and Mandelkow, E. (1992). Mitogen activated protein (MAP) kinase transforms tau protein into an Alzheimer-like state. EMBO J. *11*, 2131–2138.

Drubin, D.G., Feinstein, S.C., Shooter, E.M., and Kirschner, M.W. (1985). Nerve growth factor-induced neurite outgrowth in PC-12 cells involves the coordinate induction of microtubule assembly and assembly promoting factors. J. Cell Biol. *101*, 1799–1807.

Evans, L., Mitchison, T., and Kirschner, M. (1985). Influence of the centrosome on the structure of nucleated microtubules. J. Cell Biol. *100*, 1185–1191.

Gildersleeve, R.F., Cross, A.R., Cullen, K.E., Fagan, A.P., and Williams, R.C. (1992). Microtubules grow and shorten at intrinsically variable rates. J. Biol. Chem. *267*, 7995–8006.

Gotoh, Y., Nishida, E., Matsuda, S., Shiina, N., Kosako, H., Shiokawa, K., Akiyama, T., Ohta, K., and Sakai, H. (1991). In vitro effects on microtubule dynamics of purified *Xenopus* M phase-activated MAP kinase. Nature *349*, 251–254.

Grundke-Iqbal, I., Iqbal, K., Tung, Y., Quinlan, M., Wisniewski, H.M., and Binder, L.I. (1986). Abnormal phosphorylation of the microtubule-associated protein τ (tau) in Alzheimer cytoskeletal pathology. Proc. Natl. Acad. Sci. USA *83*, 4913–4917.

Haycock, J.W., Ahn, N.G., Cobb, M.H., and Krebs, E.G. (1992). ERK1 and ERK2, two microtubule-associated protein 2 kinases, mediate the phosphorylation of tyrosine hydroxylase at serine-31 in situ. Proc. Natl. Acad. Sci. USA *89*, 2365–2369.

Hilbush, B.S., and Levine, J.M. (1991). Stimulation of a Ca(2+)-dependent protein kinase by GM1 ganglioside in nerve growth factor-treated PC12 cells. Proc. Natl. Acad. Sci. USA *88*, 5616–5620.

Hill, T.L., and Carlier, M.-F. (1983). Steady-state theory of the interference of GTP hydrolysis in the mechanism of microtubule assembly. Proc. Natl. Acad. Sci. USA *80*, 7234–7238.

Himmler, A., Drechsel, D., Kirschner, M.W., and Martin, D.J. (1989). Tau consists of a set of proteins with repeated C-terminal microtubule-binding domains and variable N-terminal domains. Mol. Cell. Biol. *9*, 1381–1388.

Horio, T., and Hotani, H. (1986). Visualization of the dynamic instability of individual microtubules by dark-field microscopy. Nature *321*, 605–607.

Hyman, A.A. (1991). Preparation of marked microtubules for the assay of the polarity of microtubule-based motors by fluorescence. J. Cell Sci. Suppl. *14*, 125–127.

Hyman, A., Drechsel, D., Kellogg, D., Salser, S., Sawin, K., Steffen, P., Wordeman, L., and Mitchison, T. (1991). Preparation of modified tubulins. Methods Enzymol. *196*, 478–485.

Hyman, A.A., Salser, S., Drechsel, D.N., Unwin, N., and Mitchison, T.J. (1992). Role of GTP hydrolysis in microtubule dynamics: information from a slowly hydrolyzable analogue, GHPCPP. Mol. Bio. Cell *3*, 1155–1167.

Kirschner, M.W., and Mitchison, T.J. (1986). Beyond self assembly: from microtubules to morphogenesis. Cell *45*, 329–342.

Knops, J., Kosik, K.S., Lee, G., Pardee, J.D., Cohen, G.L., and McConlogue, L. (1991). Overexpression of tau in a nonneuronal cell induces long cellular processes. J. Cell Biol. *114*, 725–733.

Koshland, D., Mitchison, T.J., and Kirschner, M.W. (1988). Chromosome movement driven by microtubule depolymerization in vitro. Nature *311*, 499–504.

Landreth, G.E., Smith, D.S., McCabe, C., and Gittinger, C. (1990). Characterization of a nerve growth factor-stimulated protein kinase in PC12 cells which phosphorylates microtubule-associated protein 2 and pp250. J. Neurochem. *55*, 514–523.

Lichtenberg-Kraag, B., Mandelkow, E.-M., Biernat, J., Steiner, B., Schröter, C., Gustke, N., Meyer, H.E., and Mandelkow, E. (1992). Phosphorylation-dependent epitopes of neurofilament antibodies on tau protein and relationship with Alzheimer tau. Proc. Natl. Acad. Sci. USA *89*, 5384–5388.

Lindwall, G., and Cole, R.D. (1984a). Phosphorylation affects the ability of tau protein to promote microtubule assembly. J. Biol. Chem. *259*, 5301–5305.

Lindwall, G., and Cole, R.D. (1984b). The purification of tau protein and the occurrence of two phosphorylation states of tau in brain. J. Biol. Chem. *259*, 12241–12245.

Mandelkow, E.M., and Mandelkow, E. (1991). Microtubule dynamics and microtubule caps: a time resolved cryo-electron microscopy study. J. Cell Biol. *114*, 977–992.

Mitchison, T.J. (1984). Microtubule assembly nucleated by isolated centrosomes. Nature *312*, 232–236.

Mitchison, T.J., and Kirschner, M.W. (1984). Dynamic instability of microtubule growth. Nature *312*, 237–242.

Murphy, D.B., Johnson, K.A., and Borisy, G.G. (1977). Role of tubulin-associated proteins in microtubule nucleation and elongation. J. Mol. Biol. *117*, 33–52.

Nose, P.S., Griffith, L.C., and Schulman, H. (1985). Ca^{2+}-dependent phosphorylation of tyrosine hydroxylase in PC12 cells. J. Cell Biol. *101*, 1182–1190.

O'Brien, E.T., Salmon, E.D., Walker, R.A., and Erickson, H.P. (1990). Effects of magnesium on the dynamic instability of individual microtubules. Biochemistry *29*, 6648–6656.

O'Brien, E.T., Voter, W.A., and Erickson, H.P. (1987). GTP hydrolysis during microtubule assembly. Biochemistry *26*, 4148–4156.

Sachs, L. (1984). Applied Statistics, 2nd ed. New York: Springer-Verlag.

Savage, C., Hamelin, M., Culotti, J.G., Coulson, A., Albertson, D.G., and Chalfie, M. (1989). mec-7 is a beta-tubulin gene required for the production of 15-protofilament microtubules in *Caenorhabditis elegans*. Genes Dev. *3*, 870–881.

Schlistra, M.J., Martin, S.R., and Bayley, P.M. (1987). On the relationship between nucleotide hydrolysis and microtubule assembly: studies with a GTP-regenerating system. Biochem. Biophys. Res. Commun. *147*, 588–594.

Schulze, E., and Kirschner, M.W. (1986). Microtubule dynamics in interphase cells. J. Cell Biol. *102*, 1020–1031.

Steiner, B., Mandelkow, E.M., Biernat, J., Gustke, N., Meyer, H.E., Schmidt, B., Mieskes, G., Soling, H.D., Drechsel, D., and Kirschner, M.W. (1990). Phosphorylation of microtubule-associated protein tau: identification of the site for Ca2(+)-calmodulin dependent kinase and relationship with tau phosphorylation in Alzheimer tangles. EMBO J. *9*, 3539–3544.

Stewart, R.J., Farrell, K.W., and Wilson, L. (1990). Role of GTP hydrolysis in microtubule polymerization: evidence for a coupled hydrolysis mechanism. Biochemistry *29*, 6489–6498.

Studier, F.W., Rosenberg, A.H., Dunn, J.J., and Dubendorff, J.W. (1990). Use of T7 RNA polymerase to direct expression of cloned genes. Methods Enzymol. *185*, 60–89.

Summers, K.R., and Kirschner, M.W. (1979). Characteristics of the polar assembly and disassembly of microtubules observed in vitro by darkfield light microscopy. J. Cell Biol. *83*, 205–217.

Tsao, H., Aletta, J.M., and Greene, L.A. (1990). Nerve growth factor and fibroblast growth factor selectively activate a protein kinase that phosphorylates high molecular weight microtubule-associated proteins. Detection, partial purification, and characterization in PC12 cells. J. Biol. Chem. *265*, 15471–15480.

Ueda, K., Masliah, E., Saitoh, T., Bakalis, S.L., Scoble, H., and Kosik, K.S. (1990). Alz-50 recognizes a phosphorylated epitope of tau protein. J. Neurosci. *10*, 3295–3304.

Walker, R.A., O'Brien, E.T., Pryer, N.K., Sobeiro, M.F., Voter, W.A., Erickson, H.P., and Salmon, E.D. (1988). Dynamic instability of individual microtubules analysed by video light microscopy: rate constants and transition frequencies. J. Cell Biol. *107*, 1437.

Walker, R.A., Pryer, N.K., and Salmon, E.D. (1991). Dilution of individual microtubules observed in real time in vitro: evidence that the cap size is small and independent of elongation rate. J. Cell Biol. *114*, 73–82.

Weingarten, R.C., Lockwood, A.H., Huo, S.Y., and Kirschner, M.W. (1975). A protein factor essential for microtubule assembly. Proc. Natl. Acad. Sci. USA *73*, 1858–1862.

Yamada, K.M., Spooner, B.S., and Wessells, N.K. (1970). Axon growth: role of microfilaments and microtubules. Proc. Natl. Acad. Sci. USA *66*, 1206–1212.